# Development of a general Organic Rankine Cycle simulation tool: ORCSim

***D. Ziviani [a], B.J. Woodland [b], E. Georges [c], E.A. Groll [b], J.E. Braun [b], W.T. Horton [b], M. De Paepe [a], M. van den Broek [a]***

*[a] Department of Flow, Heat and Combustion Mechanics, Ghent University, Ghent, Belgium, davide.ziviani@ugent.be, michel.depaepe@ugent.be, martijn.vandenbroek@ugent.be*
*[b] School of Mechanical Engineering, Ray W. Herrick Laboratories, Purdue University, West Lafayette (IN), USA, bwoodlan@purdue.edu , groll@purdue.edu , jbraun@purdue.edu , wthorton@purdue.edu*
*[c] Aerospace and mechanical Engineering Department, Energy Systems, University of Liege, Liege, Belgium, emeline.georges@ulg.ac.be*

**Abstract:**

This paper presents a generalized framework for simulating steady-state performance of organic Rankine cycles named ORCSim. A Basic ORC (with or without internal regeneration) and an ORC with liquid-flooded expansion (ORC) are the current cycle configurations implemented. The overall architecture of the simulation code is described and an introduction of the individual component models is also provided. Emphasis is given to the solution algorithm, which is based on the subcooling level or the total fluid charge of the system, and improvements compared to existing models. The thermo-physical properties have been integrated by means of a wrapper, which couples the CoolProp library with flooding medium properties, typically lubricants. Both the simulation code and the graphical user interface (GUI) have been developed in the Python programming language and it will be released as fully open-source. Finally, an example of the ORCSim capabilities is shown by performing two simulations.

**Keywords:**

Organic Rankine cycle, flooded-expansion, simulation tool, GUI.

# 1. Introduction

In recent years, the simulation and optimization of organic Rankine cycles (ORCs) are of great interest especially because of an increased focus toward more environmentally-friendly energy systems. Waste heat recovery, geothermal, and solar energy represent the majority of current ORC applications on the market. Because of the variety of boundary conditions of heat sources and cold sinks, as well as working fluids, the modelling of ORCs becomes of vital importance. Often it is not feasible to perform extended experimental campaigns, especially for larger size systems.

By considering for example the ScienceDirect[1] website as a source, it is possible to draw general considerations regarding the published articles on ORCs and more specifically, modelling and simulations performed by a number of researchers. In Fig. 1, the number of publications per year is presented for several keywords.

In many cases, the models have been developed for a specific case study (or a few case studies) and by adopting one approach, i.e. simple cycle analysis [1], pinch point analysis [2], second law analysis [3], cycle optimization [4], thermo-economic analysis [5-6], dynamic modelling [7] etc. One of the shortcomings of models presented in the literature is the fact that the developed simulation tools are often only available within the research group and/or industrial partners and not in the public domain. Similar considerations were outlined by Bell et al. [8] concerning the simulation of positive displacement compressors and expanders. Furthermore, despite the global market for ORCs, to the

[1] Science Direct, Elsevier - http://www.sciencedirect.com/

authors' knowledge, there is only one package, Cycle-Tempo, in the commercial software ASIMPTOTE[2], which includes the possibility to simulate and optimize ORC systems.

The authors also acknowledge a few simulation packages available online and developed by academic researchers. For example, the Thermodynamics Laboratory at University of Liege created two significant tools: "SimORC" for the steady state simulation of ORC based on EES (Engineering Equation Solver) featuring a Graphical User Interface (GUI)[3] and "Thermocycle" an open-source Modelica based library for the dynamic simulation of ORC systems[4].

In this paper, a generalized organic Rankine cycle framework developed in the Python programming language is proposed along with the description of the modelling approaches and improvements with respect to existing models. Due to the large increase of interest in ORC systems, the aim is to introduce to the research community an ORC simulation tool which will be available online as fully open-source, allowing many users to take full advantage of the software capabilities.. The idea is to provide a platform where researchers will improve and extend the software.

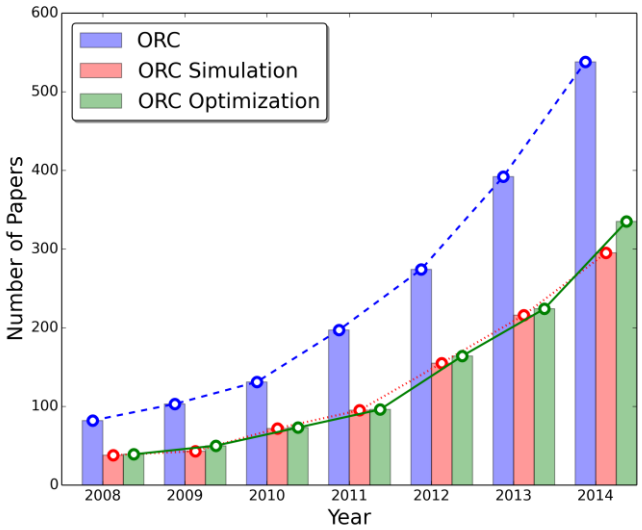


*Fig. 1. Number of publications dealing with ORC for several keywords (source: ScienceDirect, Elsevier).*

# 2. Organic Rankine Cycle SIMulation tool: ORCSim

## 2.1. Framework overview

The framework developed, i.e. ORCSim, aims to become a generalized platform for the simulation and optimization of ORC systems. The underlying code is adapted from ACHP[5], a modular, open-source software package for the analysis of air conditioners and heat pumps. ORCSim makes use of the same basic framework and cycle solution scheme as ACHP. Like ACHP, ORCSim is based on the idea of modularity, meaning that it allows the integration of additional analysis types and component models. A user-friendly interface and numerical stability of the software have been the main objectives in its design.

Currently, three simulation types are implemented: (i) "cycle analysis": simple thermodynamic analysis of the system useful for quick evaluation and screening purposes; (ii) "design analysis": detailed component models are integrated into a cycle solver based on subcooling level or working

[2] ASIMPTOTE - http://www.asimptote.nl/about-us/

[3] Thermodynamics Laboratory, University of Liege - http://www.labothap.ulg.ac.be/cmsms/index.php?page=orc-simulation

[4] Open-source ThermoCycle library developed in the Modelica language - http://www.thermocycle.net/

[5] Bell, I., ACHP - http://achp.sourceforge.net/

fluid charge (described in this paper); (iii) "simple optimization": on the basis of simple thermodynamic analysis, an optimization loop is implemented to determine the optimum volumetric expander size to maximize the power output or the cycle efficiency. Additional optimization capabilities will be integrated as part of future development of the software.

Focusing on (ii), four different cycle configurations are currently available in the simulation tool and they are graphically shown in Fig. 3. They include ORC with/without internal regenerator and ORC with flooded expansion (ORCLFE) with/without internal regenerator [9].

The simulation process passes through three main steps, i.e. "Inputs", where all the cycle and component parameters are specified, "Solver" which allows a selection of either a single run or a parametric study and "Outputs" to display all the results for each component and thermodynamic plots.

Due to the limit of pages, in this paper only the traditional ORC system with and without internal regenerator is described in detail. However, an example of ORCLFE analysis is discussed.

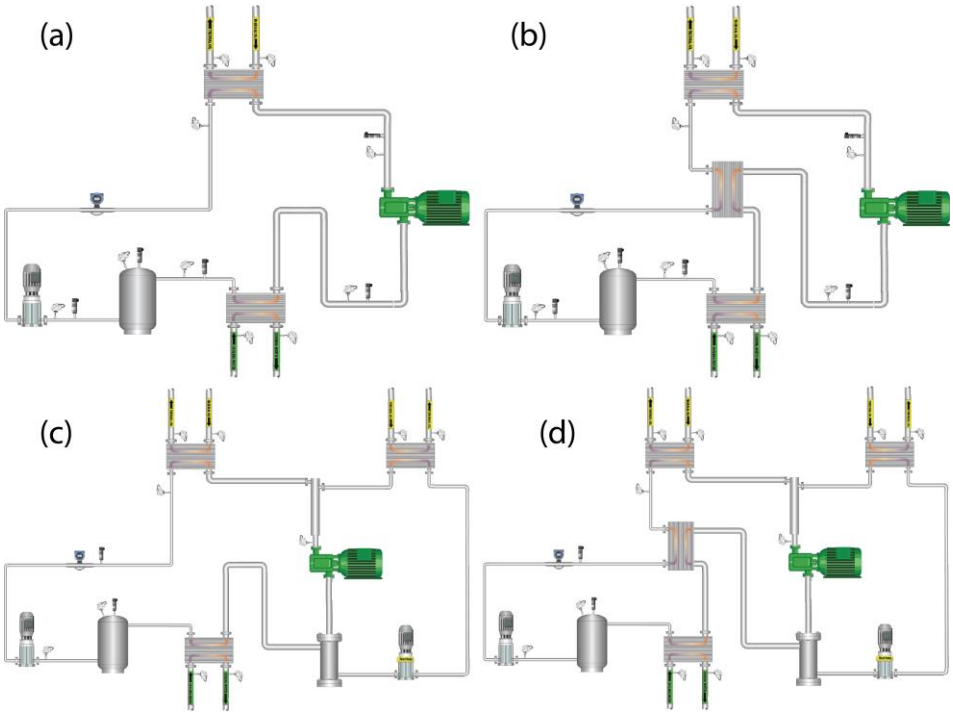


*Fig. 2. Cycle configuration available in ORCSim: ORC without/with internal heat exchanger (a-b) and ORC with flooded expansion (ORCLFE) without/with internal heat exchanger (c-d).*

## 2.2. Component models

The main ORC system configurations currently available within the software are illustrated in Fig. 2.

### 2.2.1. Plate heat exchangers

The plate heat exchangers (PHEX), i.e. evaporator, condenser and regenerator (or internal heat exchanger) have been modelled using a steady-state moving boundary approach [10] with slightly modified code from the original versions in ACHP. By considering the schematic representation of a single plate as in Fig. 3, the active area can be calculated including all the geometric characteristics. Due to the configuration of the PHEX, the modelling principle is a counter flow heat exchanger. The solution is obtained by determining first the bounding heat transfer rate, i.e. corresponding to 100% effectiveness and then, by iterating it between zero and the maximum in order to converge to the actual heat transfer rate that satisfies the geometry size of the PHEX. Mathematically, the upper bound of the heat transfer rate is expressed by:

$$\dot{Q}_{\max,\,\varepsilon=1} = \min\left[\dot{Q}_{\max,\,c}, \dot{Q}_{\max,\,h}\right], \qquad (1)$$

$$\dot{Q}_{\max,c} = \dot{m}_c\left(h_c\left[p_{c,ex}, T_{h,su}\right] - h_{c,su}\right), \qquad (2)$$

$$\dot{Q}_{\max,h} = \dot{m}_h\left(h_{h,su} - h_h\left[p_{h,ex}, T_{c,su}\right]\right). \qquad (3)$$

Physically impossible situations, such as crossing of the temperature profiles of the two fluids streams at internal pinch points, are avoided by properly expressing the maximum heat transfer rate [10]. Additionally, the process continues until all the boundaries of both sides have been calculated, in particular single-phase or two-phase zones. The convergence of the size of the heat exchanger is obtained when the sum of each zone's relative length is unity:

$$\sum_k w_k = \sum_k \frac{L_k}{L} = 1. \qquad (4)$$

The model also estimates the charge level of the working fluid based on the geometric parameters and thermodynamic properties. More details about the heat transfer and pressure drop calculations can be found in the ACHP documentation[5]. In Fig. 4, examples of the evolution of the temperature through the evaporator (left) and condenser (right) are shown.

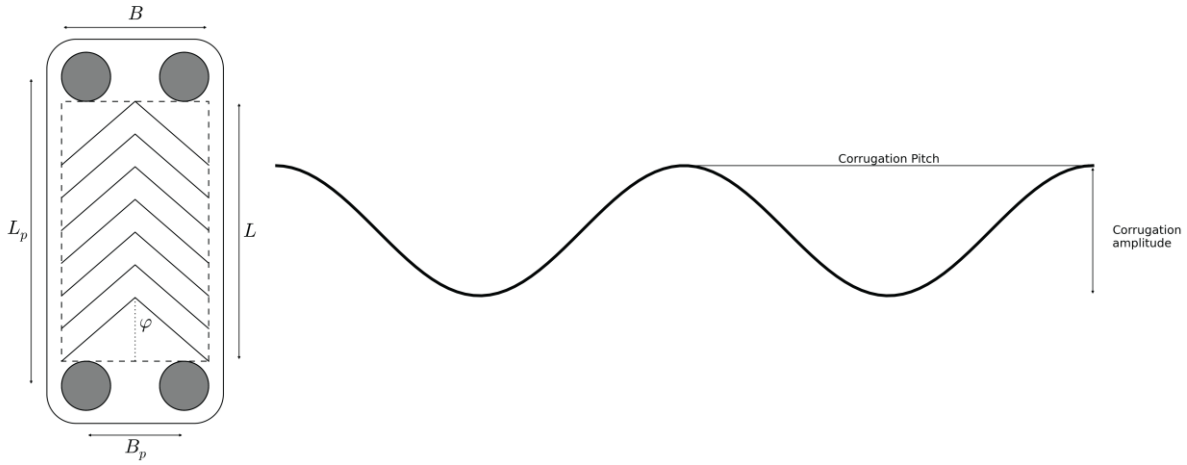


*Fig. 3. Geometric parameters of a single plate of a PHEX.*

### 2.2.2. Pump

The pump performance is characterized by general correlations fit to experimental results. By modifying the coefficients, it is possible to modify the pump type. Two approaches are considered.

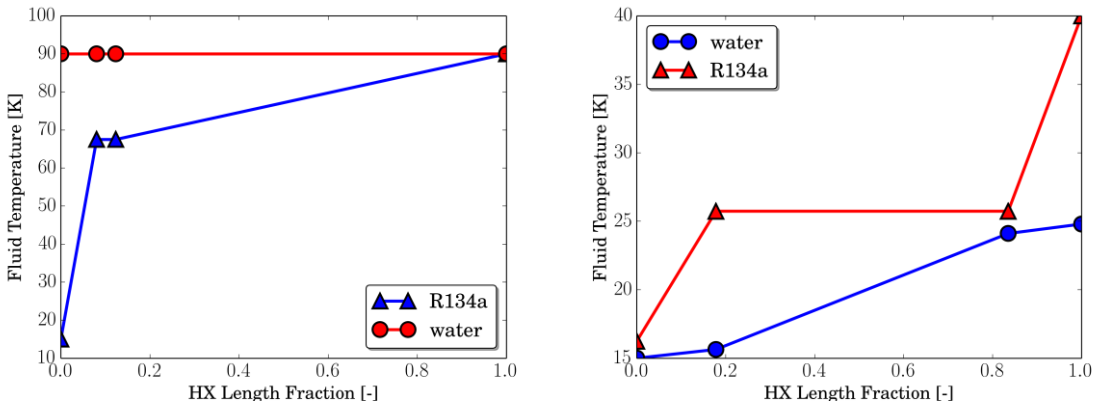


*Fig. 4. Examples of evaporator (left) and condenser (right) using steam and water as hot source and cold sink respectively and R134a as working fluid.*

The first one is based on the mass flow rate and the power consumption expressed by linear correlations of the rotational speed and pump pressures [11]. In particular,

$$\dot{m}_{calc,p} = aN_p + b, \qquad (5)$$

where a and b are each linear functions of the pump discharge pressure. The power correlation first requires that a reference speed be chosen. The reference power of the pump is a linear correlation with pump pressure difference at the chosen reference shaft speed, given as

$$\dot{W}_{p,ref} = c\Delta p_p + d\big|_{N_p = N_{p,ref}}. \qquad (6)$$

The ratio of pump power at any speed to the rated power at the pressure difference (found by equation (6)), correlates linearly to the ratio of shaft speed and the reference shaft speed. It is given by

$$\frac{\dot{W}_{calc,p}}{\dot{W}_{p,ref}} = e\frac{N_p}{N_{p,ref}} + f, \qquad (7)$$

which is solved for the calculated pump power.

The second methodology maintains a correlation for the mass flow rate but substitutes the power consumption with the isentropic effectiveness. Thus, the rotational speed is converted to a frequency. Therefore, the mass flow rate is a quadratic function of pressure difference and frequency,

$$\dot{m}_{calc,p} = a_1 + a_2\Delta p_p + a_3\Delta p_p^2 + a_4 f_p + a_5 f_p^2. \qquad (8)$$

The isentropic effectiveness is related to pressure difference, pressure ratio, frequency and density of working fluid expressed in non-dimensional terms by choosing a reference or nominal value:

$$x^* = \frac{x - x_{ref}}{x_{ref}}, \qquad (9)$$

$$\varepsilon_{s,p} = f\left(\Delta p_p^*, f_p^*, r_{p,p}^*, \rho_{p,r}^*\right), \qquad (10)$$

where $\Delta p = p_{p,ex} - p_{p,su}$ and $r_{p,p} = p_{p,ex} / p_{p,su}$.

### 2.2.3. Expander

The simulation tool includes several models for the expander. In this particular case, only positive displacement machines are considered. Currently, scroll and single-screw expanders have been implemented and it is possible to choose the type from a drop down menu. Of the four expander models implemented, one is a simple constant efficiency model. The other three are based on empirical or semi-empirical approaches. The first empirical model is a standard expander map. It is based on mass flow rate and power output and expressed in terms of polynomial functions. The coefficients can be loaded from a file or specified directly by the user. The second empirical model calculates two parameters that characterize the performance of an expander: isentropic efficiency and filling factor. The former parameter is obtained by a function of physical parameters, i.e. pressure ratio, rotational speed and supply pressure, and the equation resembles the one proposed by Pacejka and is currently used to model expander performance [12]. The latter parameter is obtained from a logarithmic type of equations still using the same physical parameters. It is recalled that the filling factor is related to the volumetric performance of the machine and gives information about leakage. It is defined as

$$\phi_{FF} = \frac{\dot{m}_r v_{r,\exp,su}(p_{r,\exp,su}, T_{r,\exp,su})}{\dot{V}_{th,\exp}}. \qquad (11)$$

By specifying the swept volume of the machine (either as compressor or expander) and the built-in volume ratio, $V_{geom,exp} = V_{geom,comp}/r_{v,built\text{-}in}$, given the filling factor correlation, the mass flow rate can be calculated. From the isentropic efficiency, the discharge states are determined and the power produced is estimated.

The last model implemented represents the semi-empirical model first proposed for an expander by Lemort et al. [13]. The expansion process is decomposed in several steps to take into account pressure drops, heat transfer, and mechanical losses. The solution is obtained by driving to zero the following overall energy balance with a fictitious lumped wall temperature:

$$\dot{Q}_{su,\exp} + \dot{Q}_{ex,\exp} + \dot{W}_{loss} - \dot{Q}_{amb} = 0 \qquad (12)$$

where

$$\dot{Q}_{amb} = AU_{amb}\left(T_w - T_{amb}\right). \qquad (13)$$

The identification of the parameters is carried out by minimizing an objective function with experimental data. The objective function could be a combination of desired model outputs such as mass flow rate, shaft power, and working fluid exit temperature. The model has also been extended to include the presence of a flooding medium, i.e. lubricant oil.

### 2.2.4. Liquid receiver

The liquid receiver in the ORC system has a dumping function absorbing the mass flow rate fluctuations (especially during dynamic tests). Moreover, similar to refrigeration cycles, the refrigerant charge has a strong influence on the subcooling at the condenser outlet. In fact, more refrigerant charge implies a higher liquid level in the heat exchangers and therefore the subcooling zone is enhanced. To maximize the ORC efficiency, the subcooling level should be maintained at a minimum for each set of operating conditions. This would require an adjustment of the refrigerant charge in practice. For these reasons, the liquid receiver is a good solution to keep the subcooling at zero over a range of refrigerant charge levels. A subcooler could be added downstream of the receiver to ensure positive subcooling at the pump inlet. Since one of the possible convergence criteria in the current model is the total refrigerant charge (see section 2.4), it is important to include the presence of this additional volume. The liquid receiver is considered to be adiabatic and its volume represents the only parameter (pressure drops at inlet/outlet are neglected). The steady-state level of the receiver is given by:

$$level = \left(\frac{h_{r,v,sat} - h_{r,su}}{h_{r,v,sat} - h_{r,l,sat}}\right)\frac{\rho_{r,su}}{\rho_{l,sat}} = \frac{m_{r,l,sat}}{m_{r,tot}}\frac{v_{l,sat}}{v_{r,su}} = \frac{V_l}{V_{tot}}. \qquad (14)$$

As outputs, the model calculates the inlet pressure, the liquid level and the refrigerant charge.

### 2.2.5. Pipelines

The piping system is also considered in the model. The pipeline connections between components are modelled as an equivalent tube with inner and outer diameters. The model includes heat transfer to the environment, internal heat transfer and pressure drop. The overall heat transfer coefficient, UA, is the sum of the thermal resistance of the tube, the thermal resistance associated with the insulation and the convective UA values associated with the inside and outside of the tube:

$$UA_{pipe} = \left(\frac{1}{UA_{ID}} + \frac{1}{UA_{OD}} + R_{tube} + R_{insulation}\right)^{-1}. \qquad (15)$$

The pressure drops are calculated for single-phase flow. As a general description, the pressure gradient along the pipe of the internal flow is obtained through the Darcy friction factor and the pressure drop can be easily obtained by multiplying the pressure gradient by the total length of the pipe:

$$\Delta p = \left(\frac{dp}{dz}\right)\cdot L = \left(-\frac{f\mathbf{v}G^2}{2\cdot ID}\right)\cdot L. \qquad (16)$$

Finally, the charge of refrigerant is estimated through the piping.

## 2.3. Thermophysical property wrapper

The simulation of the ORC requires the computation of thermophysical properties and in many cases, most of the computational time is associated with calling and estimating the properties. Furthermore, ORCSim includes the possibility of having lubricant oil in solution with the refrigerant in the ORC loop. It also allows the simulation of ORCLFE (organic Rankine cycle with liquid-flooded expansion), for which the lubricant oil properties are absolutely necessary. The thermophysical properties of the working fluids are retrieved by using either CoolProp [14] or REFPROP [15]. An adapted version of "Refprop2.py[6]" has been implemented which allows the user to call the properties with the same syntax as CoolProp as well as the same units. The possibility to call refrigerant mixture properties based on mass fraction has also been added. A property wrapper has been added to calculate both the properties of the lubricant oil and the mixture of oil and refrigerant. To simplify the analysis, the mixture has been treated as a pseudo-pure fluid, i.e. ideal mixture model. For a homogenous two-phase mixture with equal velocities, the mixture density, specific volume, constant pressure specific heat, specific internal energy, specific enthalpy and specific entropy can be calculated introducing the oil (or liquid) mass fraction, $x_L$. For example the mixture specific internal energy is given by

$$u_{mix} = x_L u_L + (1 - x_L) u_G \qquad (17)$$

The mixture thermal conductivity is defined as a void-fraction weighted average of oil and refrigerant thermal conductivities. For the mixture viscosity, the model proposed by McAdams et al. [16] is assumed.

## 2.4. Pre-conditioning and cycle solver

The individual components previously described are connected to simulate the entire cycle. The solution is reached through a single simulation pass through two consecutive steps: a solver pre-conditioner and an overall cycle solver. The pre-conditioner has the role of estimating the first guesses of the evaporating and condensing temperatures, which are required by the main solver. The guess cycle is implemented in the same way as the main cycle but the heat exchanger model is simplified by assuming an effectiveness. The solution scheme is based on two residuals which are driven to zero by the pre-conditioner solver. In particular, the residuals are the overall energy balance of the ORC system:

$$\dot{W}_p + \dot{Q}_{evap} - \dot{W}_{\exp} - \dot{Q}_{cond} = 0, \qquad (18)$$

and the difference between the mass flow rate of the pump and the expander:

$$\dot{m}_p - \dot{m}_{\exp} = 0. \qquad (19)$$

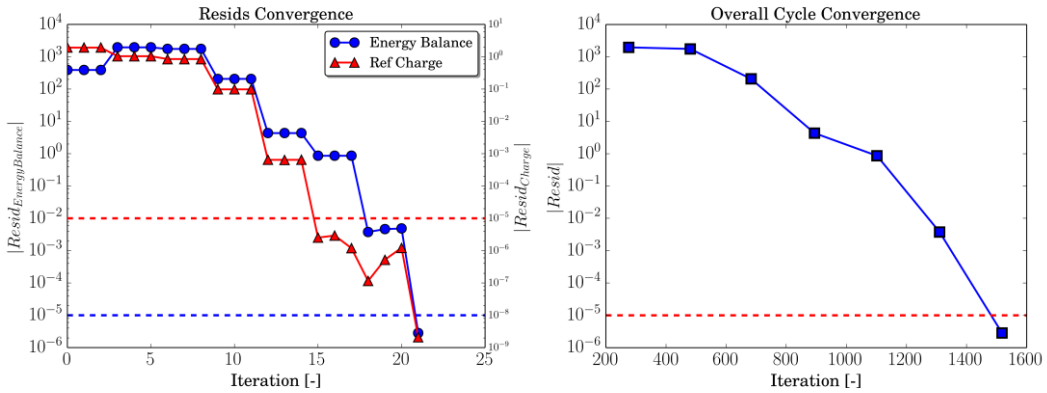


*Fig. 5. Convergence history of residuals (left) and main cycle solver (right).*

[6] Refprop.py and Refprop2.py created by Bruce Wernick - http://www.boulder.nist.gov/div838/theory/refprop/WERNICK.ZIP#REFPROP2.PY-38k-2012-10-29

Once the pre-conditioner residuals converge, the set of guessed values is used to launch the main solver to actually execute the simulation. The calculation proceeds by minimizing two additional residuals by means of a multi-variable Newton-Raphson algorithm. One residual is equivalent to the energy balance (12) and the other one can be selected by the user from the main cycle tab. In particular, either the subcooling (i) or the total refrigerant charge (ii) can be used as convergence criteria, depending on the requirements of the simulation,

i. $\Delta T_{sub,calc} - \Delta T_{sub,input} = 0$, (20)

ii. $m_{r,ORC,calc} - m_{r,ORC,input} = 0$. (21)

where:

$$m_{r,ORC,calc} = m_{r,evap} + m_{r,cond} + \sum_i m_{r,pipeline,i} + m_{r,\exp} + m_{r,p} \quad (22)$$

By selecting one of the two criteria, the other variable is given as result of the simulation. The convergence history is given in the solver tab and the charts can be saved as images, as shown in Fig. 5. The computational time is also an output. In the solver tab, it is also possible to perform a parametric analysis. Up to four variables can be selected to run multiple simulations by specifying the lower and upper limits and the number of steps to be taken. After the simulations are completed, the results are saved in a spreadsheet file.

# 3. Implementation, GUI and novelty

The cycle simulation has been coded in the Python programming language[7] by taking advantage of its object-oriented programming environment, which allows a high level of modularity as well as high computational performance. In particular, it is quite easy to integrate additional components or models into the overall cycle without impacting the structure of the core of the code. This approach is instrumental in enabling users to expand and improve the open-source code. The Graphical User Interface (GUI) of ORCSim has been developed using the open-source package "wxPython" along with "wxFormBuilder". The executable has been created with "cxFreeze" by creating a proper setup file and the installation wizard is obtained by "Inno Setup Compiler". One feature regarding the GUI that has to be mentioned is the possibility of saving/loading a configuration file. All the parameters introduced in a simulation can be automatically stored in a text-type of file. By modifying the configuration file, it is possible to load the new values into the next simulation, speeding the process.

ORCSim begins to address several limitations that are often encountered with other simulation models proposed in the literature. At the component level, the PHEX model is able to handle a wide range of fluids including refrigerants, zeotropic mixtures, incompressible fluids, thermal oils, lubricant oils and two-phase mixtures for both sides. Currently, two types of expanders are included with different models having different complexities. At the system level, the cycle model allows the investigation of an ORC with liquid-flooded expansion and internal regeneration. In order to simulate this novel cycle architecture the expander semi-empirical model had to be adapted to include the flooding medium and two-phase flow conditions. The solution scheme of the cycle allows the selection of two different converging criteria: subcooling level or charge level. Meanwhile the former one is more commonly implemented, the latter one, to the authors' knowledge, is less considered because of the difficulties in estimating the total charge. However, the optimization of the refrigerant charge is a key aspect during the operation of the ORC. The simulation tool estimates the charge of each component (simplifications have been introduced for the expander and pump) and the solver drives to zero the residuals of the overall cycle energy balance and the difference between the imposed and calculated refrigerant charge. The influence of the charge level on the system performance can then be investigated.

[7] Python programming language - https://www.python.org/

*Table 1. Example of application of ORCSim to an ORC test rig and comparison between experimental data and calculated values.*

| | *Type* | *Measured/imposed* | *Calculated* |
|---|---|---|---|
| Working fluid | R134a | - | - |
| ORC charge, kg(lb) | - | 5.44(12) | - |
| Hot source | Steam | - | - |
| Hot source inlet temperature, °C | - | 104.94 | - |
| Cold sink | Water | - | - |
| Cold sink inlet temperature, °C | - | 15.51 | - |
| Expander | Reversed scroll compressor | - | - |
| Expander model | Semi-Empirical | - | - |
| Compressor swept volume, $cm^3$ | - | 104.8 | - |
| Built-in volume ratio, - | - | 1.8 | - |
| Subcooling, °C | - | 9.32 | 10.83 |
| Expander isentropic efficiency, - | - | 0.7158 | 0.6974 |
| Working fluid mass flow rate, kg/s | - | 0.1632 | 0.1625 |
| ORC thermodynamic efficiency, - | - | 0.0584 | 0.0637 |

# 4. Examples of ORCSim capabilities

After the simulation converges, results are given both at the component level and as cycle performance indicators, i.e. thermodynamic and global ORC efficiencies, Second-Law efficiency, back work ratio (BWR). For instance, the global efficiency is defined as the product of the heat recovery ratio (HRR), which is important in waste heat recovery applications, and the thermodynamic efficiency of the ORC. Mathematically the relationship is expressed by:

$$\eta_{global} = \frac{\dot{W}_{net,ORC}}{\dot{Q}_{available}} = \frac{\dot{W}_{net,ORC}}{\dot{Q}_{recovered}} \frac{\dot{Q}_{recovered}}{\dot{Q}_{available}} = \eta_{ORC} \cdot \eta_{HRR}, \quad (23)$$

where $\dot{Q}_{available}$ is the total amount of thermal power if the hot source would have been cooled down to ambient temperature.

The plot capabilities of ORCSim include T-s diagrams, as shown in Fig. 6 and p-h thermodynamic plots as well as the temperature profile through the heat exchangers, as previously illustrated in Fig. 4. All the results can be exported to a file. The numerical example proposed throughout the paper is based on experimental data obtained from the ORC test rig installed at the Herrick Laboratories, Purdue University and the main test case inputs are listed in Table 1. The simulation has been carried out based on the charge level and the subcooling is then obtained as a result. The imposed convergence tolerance is $10^{-5}$ for all the residuals as previously shown in Fig. 5. One of the major results of this type of analysis is the influence of the refrigerant charge on the subcooling. Good performance of the ORC is related to correct estimation of the charge level and this fact is of extreme importance for real applications. Often it is difficult to evaluate directly the impact of the refrigerant charge because it requires detailed modelling of the components. The present simulation tool overcomes this limitation in part by implementing detailed models for each of the components. Although some approximations are introduced, for instance the refrigerant charge estimation for the pump and expander, ORCSim represents an improvement over existing ORC models.

The detailed modelling of the ORC system allows the investigation of the influence of different parameters. Of particular interest, for example, is the selection of the expander in terms of built-in volume ratio. It is well known that, ideally, the maximum expander efficiency should correspond to the maximum cycle efficiency, meaning that the expander is a perfect match for the given working fluid and operating conditions. Often, positive displacement expanders are simply reversed compressors, which can result in a poor match with the operating conditions. A parametric study for

example can be carried out to evaluate the impact of the built-in volume ratio, $r_{v,in}$, of a scroll expander under flooded-expansion, i.e. ORCLFE [9,11]. The flooded-expansion allows to obtain a quasi-isothermal expansion with a consequent increase in work produced compared to the corresponding adiabatic one. The presence of a significant amount of oil in the working chamber modifies the volume ratio seen by the refrigerant. In particular an effective built-in volume ratio can be defined as follows:

$$r_{v,in}^{*} = \frac{r_{v,in} - a_l}{1 - a_l} = \frac{r_{v,in} - \left(V_{oil,su}/V_{s,\exp}\right)}{1 - \left(V_{oil,su}/V_{s,\exp}\right)}, \qquad (24)$$

where $a_l$ represents the ratio between the volume of liquid (typically oil) at the expander inlet and the expander displacement. As shown in Fig. 7(left), the higher the oil volume fraction, the higher the effective built-in volume ratio. Also, in order for the oil to have a significant effect on the volume ratio, the original built-in volume ratio should be greater than 4. By considering as a reference case the data listed in Tab. 1, the built-in volume ratio is increased by fixing the operating conditions. The ratio between oil and refrigerant mass flow rates, $y$, is fixed in this case at 0.30. A parametric analysis has been carried out with ORCSim in order to determine the internal volume ratio that maximizes both the isentropic efficiency and the cycle efficiency. The result of the analysis is shown in Fig. 7(right).

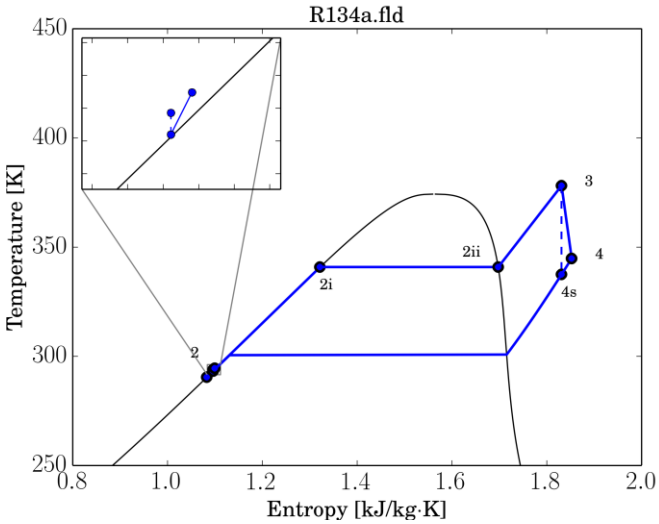


*Fig. 6. Cycle T-s plot capabilities of ORCSim.*

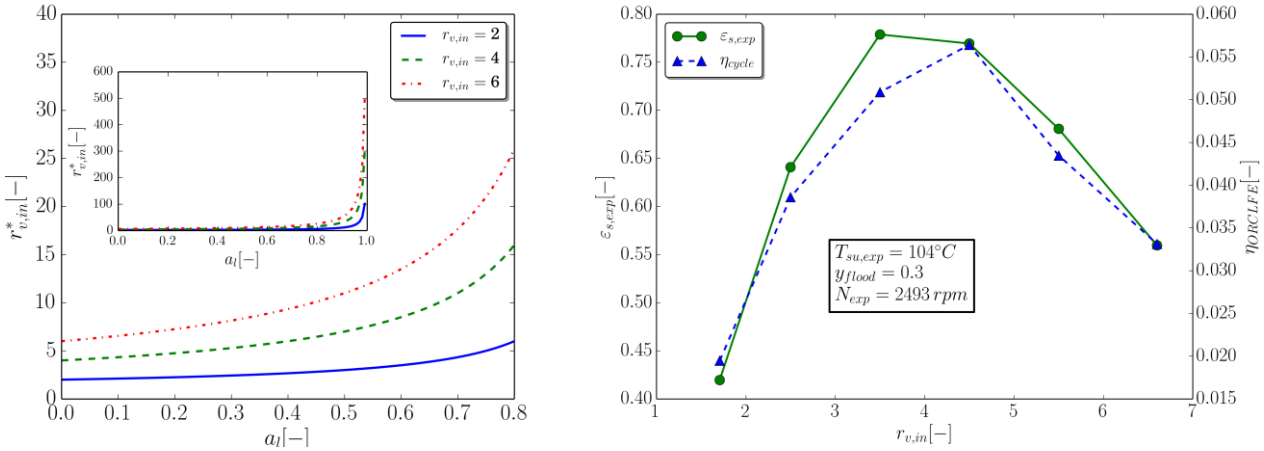


*Fig. 7. Influence of the ratio of oil volume to expander displacement on the effective built-in volume ratio (left); parametric analysis of different built-in volume ratios on the expander and ORC performance at fixed operating conditions (right).*

The benefits of flooded expansion are related to the internal built-in volume ratio. For a given flooding ratio, there exists an optimum volume ratio that maximizes the cycle efficiency, in this case close to 4.5. Alternatively, for each built-in volume ratio there exists an optimum flooding ratio that allows to improve the cycle efficiency compared to the baseline ORC. Finally, the computational time is directly related to the boundary conditions and the type of model selected. The heat exchanger and performance map models run in fractions of a second. The cycle simulation varies between a minute up to several minutes.

# 5. Conclusion

The development of a generalized framework for the simulation of organic Rankine cycles has been presented. The software package named ORCSim allows the simulation of the steady-state performance of ORC systems. The structure of the tool and the main components have been described. The code and the GUI have been implemented entirely in Python. Because of its highly object-orientated nature, the code can be easily modified and extended with additional components and simulation packages. Finally, examples of the outcomes have also been included.

# Acknowledgments

The authors would like to acknowledge Ian H. Bell for the precious advice he offered on countless occasions during the development of the software.

# Nomenclature

| | | | |
|---|---|---|---|
| $G$ | mass flux, kg/(s m$^2$) | $\dot{Q}$ | heat rate, W |
| $h$ | specific enthalpy, J/kg | $r_{v,in}$ | Built-in volume ratio, (-) |
| $L$ | length, m | $u$ | specific internal energy, J/kg |
| $m$ | mass, kg | $v$ | specific volume, m$^3$/kg |
| $\dot{m}$ | mass flow rate, kg/s | V | Volume, m$^3$ |
| $p$ | pressure, Pa | $\dot{V}$ | volumetric flow rate, m$^3$/s |
| $T$ | temperature, °C | $\dot{W}$ | power, W |

### Greek symbols

| | |
|---|---|
| $\eta$ | efficiency |
| $\rho$ | density |
| $\varepsilon$ | effectiveness |
| $\phi_{FF}$ | filling factor |

### Subscripts and superscripts

| | | | |
|---|---|---|---|
| amb | Ambient | ORCLFE | Organic Rankine Cycle with Liquid-Flooded Expansion |
| c | cold | p | pump |
| calc | calculated | r | refrigerant |
| cond | condenser | ref | reference |
| ex | exhaust | su | supply |
| exp | expander | tot | total |
| h | hot | V | vapour |
| l | liquid | | |
| mix | mixture | | |
| ORC | Organic Rankine Cycle | | |

## References


[1] Quoilin S., Lemort V., Lebrun J., "Experimental study and modelling of an Organic Rankine Cycle using scroll expander". Applied Energy 2010;87(-):1260-68.

[2] Guo C., Du X., Yang L., Yang Y., Performance analysis of organic Rankine cycle based on location of heat transfer pinch point in evaporator. Applied Thermal Engineering 2014;62(1):176-186.

[3] Tchanche B.F., Lambrinos Gr., Frangoudakis A., Papadakis G., Exergy analysis of micro-organic Rankine power cycles for a small scale solar driven reverse osmosis desalination system. Applied Energy 2010;87(-):1295-1306.

[4] Maraver D., Royo J., Lemort V., Quoilin S., Systematic optimization of subcritical and transcritical organic Rankine cycles (ORCs) constrained by technical parameters in multiple applications. Applied Energy 2014;117(-):11-29.

[5] Quoilin S., Declaye S., Tchanche B.F., Lemort V., Thermo-economic optimization of waste heat recovery Organic Rankine Cycles. Applied Thermal Engineering 2011;31(-):2885-93.

[6] Lecompte S., Huisseune H., van den Broek M., De Schampheleire S., De Paepe M., Part load based thermo-economic optimization of the Organic Rankine Cycle (ORC) applied to a combined heat and power (CHP) system. Applied Energy 2013;111(-):871-81.

[7] Quoilin S., Bell I.H., Desideri A., Lemort V., Methods to increase the robustness of finite-volume flow models in thermodynamic systems. Energies 2014;7(3):1621-40.

[8] Bell I.H, Lemort V., Groll E.A., Braun J.E., Horton W.T., Development of a generalized steady-state simulation framework for positive displacement compressors and expanders. ICCS 2013: Proceedings of the 8th International Conference on Compressors and their Systems; 2013 September 9-10; London, UK. Woodhead Publishing: 717-29.

[9] Woodland B.J., Krishna A., Groll E.A., Braun J.E., Horton W.T., Garimella S.V., Thermodynamic comparison of organic Rankine cycles employing liquid-flooded expansion or a solution circuit. Applied Thermal Engineering 2013;61(-):859-65.

[10] Bell I.H., Quoilin S., Georges E., Braun J.E., Groll, E.A., Horton W.T., Lemort V., A generalized moving-boundary algorithm to predict the heat transfer rate of counterflow heat exchangers for any phase configuration. Applied Thermal Engineering 2015;79(-):192-201.

[11] George E., Investigation of a Flooded Expansion Organic Rankine Cycle system [Master Thesis]. Liege, Belgium: University of Liege; 2012.

[12] Declaye S., Quoilin S., Guillaume L., Lemort V., Experimental study on an open-drive scroll expander integrated into an ORC (Organic Rankine Cycle) system with R245fa as working fluid. Energy 2013;55(-):173-183.

[13] Lemort V., Quoilin S., Cuevas C., Lebrun J., Testing and modelling a scroll expander integrated into an Organic Rankine Cycle. Applied Thermal Engineering 2009;29(-):3094-102.

[14] Bell I.H., Wronski J., Quoilin S., Lemort V., Pure and pseudo-pure fluid thermophysical property evaluation and the open-source thermophysical property library CoolProp. Industrial Engineering Chemistry Research 2014;53:2498-508.

[15] Lemmon E.W., Huber M.L., McLinden M.O., NIST Standard Reference Database 23: Reference Fluid Thermodynamic and Transport Properties-REFPROP, Version 9.1. National Institute of Standards and Technology, Standard Reference Data Program, Gaithersburg, 2013.

[16] McAdams W., Wood W., Bryan R., Vaporization inside Horizontal Tubes – II: Benzene-oil mixtures. Transactions ASME 1942; 64(-):193.